INVESTIGATION OF T6 HEAT TREATMENT ON DRY SLIDING WEAR BEHAVIOUR OF THIXOFORMED A356 COMPOSITE REINFORCED WITH GRAPHENE

N.F.B.W. Anuar[1,2], M.Z. Omar[1], M.S. Salleh[2*], S.H. Yahaya[2], S. Al-Zubaidi[3]

[1]Faculty of Engineering and Built Environment, Universiti Kebangsaan Malaysia, UKM Bangi, 43600 Selangor, Malaysia

[2]Fakulti Teknologi Dan Kejuruteraan Industri Dan Pembuatan, Universiti Teknikal Malaysia Melaka, Hang Tuah Jaya, Durian Tunggal Melaka, 76100 Melaka, Malaysia

[3]Al-Khwarizmi College of Engineering, University of Baghdad, 10071 Baghdad, Iraq

*Corresponding Author's Email: shukor@utem.edu.my

Article History: Received 15 January 2024; Revised 12 June 2024; Accepted 10 July 2024

ABSTRACT: Improving the wear resistance of graphene reinforced aluminium matrix composites is essential to broaden its application range, notably in high-abrasive environments. Introducing the heat treatment process to graphene reinforced aluminium metal matrix composites potentially resulted in an enhancement in hardness properties and led to an increase in its wear resistance. Thus, this study investigates the impact of the T6 heat treatment on the hardness and wear behaviour of thixoformed GNPs-A356 composites. The GNPs-A356 aluminium composites were produced via the stir casting route in preparation for the subsequent thixoforming process. The feedstock of the composites was reheated to 50% liquid fraction temperature, as identified from the DSC analysis graph, before being rammed into the mould. The thixoformed composites underwent the standard T6 heat-treatment technique. The microstructure of the heat-treated composites shows a formation of spheroidal Si. The addition of GNPs significantly affected the microstructure after the thixoforming process and increased the hardness values from 63 HV for the A356 alloy to 95.39 HV for the thixoformed composite. The following T6 heat treatment process increases the hardness

value to 107.45 HV. The volume loss, specific wear rate and average friction of heat-treated GNPs-A356 composites decreased approximately by 28.9 %, 28.7 % and 5.5 %, respectively, compared to A356 alloy. The T6 heat treatment significantly promotes the positive impacts on the properties of hardness and dry sliding wear behaviour of the thixoformed composites.

KEYWORDS: *Graphene Nanoplatelets; Aluminium Metal Matrix Composites; Thixoforming Process; Heat Treatment; Dry Sliding Wear Behaviour*

1.0 INTRODUCTION

Recent research indicates that aluminium and its alloys are extensively recognised for their advantages, including being lightweight, cost-effective, durable, processing capability, and wear resistance [1]. Consequently, its potential applications in automotive, aerospace, and other industries have expanded. However, the inherently limited durability of aluminium alloys prevents them from fulfilling the progressively demanding industrial manufacturing standards. Thus, the employment of reinforcement particles in the aluminium matrix enhances its ability to be used in advanced technological applications.

Researchers have introduced a diversity of reinforcement materials to enhance the wear properties of aluminium matrix composites, such as SiC [2], B_4C [3], Al_2O_3 [4], and ZrO_2 [5]. This is owing to the capability of self-lubricating from the reinforcement materials, which reduced the composites' friction and wear rate. Carbon materials such as graphene [1], carbon nanotubes [6] and graphite [7] are frequently employed as reinforcement materials because of their ability to enhance the resistance to wear through their self-lubricating capabilities. Graphene comprises sp^2-hybridized carbon atoms arranged in a single atomic layer [8]. Graphene has also garnered significant research attention because of its exceptional characteristics, such as outstanding heat conductivity, excellent mechanical characteristics and exceptional self-lubricating effects [9, 10].

Powder metallurgy and casting are the primary methods for fabricating graphene-reinforced aluminium metal matrix composites. The casting process is preferred for large-scale industrial production over powder metallurgy due to its complex processing and higher costs. In addition, the casting process can produce complex components owing to its simple equipment requirements and low costs [11]. Furthermore, applying the thixoforming process as a secondary

process can strengthen the structure and characteristics of the as-cast aluminium metal matrix composite. Currently, implementing the heat treatment technique is worthwhile as it simultaneously enhances the mechanical characteristics, including the wear behaviour of aluminium matrix composites. This is due to the heat treatment process significantly influencing the characteristics and microstructure to meet specific application requirements [12, 13]. Numerous studies have established the successful use of T6 heat treatment to enhance the mechanical properties of aluminium. Wang et al. [14] found that the tensile strength and hardness are reduced after the T6 heat treatment process due to coarsening of microstructure and slow cooling rate, resulting in a change in the strengthening mechanism. However, the addition of carbon reinforcement potentially increases the nucleation of the required intermetallic phase and is beneficial in preventing coarser microstructure in the composites during the heat treatment process [15].

Nevertheless, the impact of the heat treatment process on the characteristics of graphene-reinforced aluminium metal matrix composites still needs to be explored. Therefore, this study investigates the impacts of T6 heat treatment on the characterisation of thixoformed A356–0.3 wt.% GNP composites. The stir casting and thixoforming processes were used to fabricate A356–0.3 wt.% GNP composites before undergoing T6 heat treatment. A comprehensive analysis was conducted to examine the characteristics of microstructure, hardness, and dry sliding wear of the fabricated composite.

2.0 METHODOLOGY

2.1 Fabrication of composites

The detailed composition information of the A356 alloy was verified using a SPECTROMAXx arc/spark optical emission spectrometry (OES) analyser, and the element compositions are shown in Table 1.

Table 1: Weight percentage (%) of the elements composition of the A356 alloy

Si	Mg	Cu	Ni	Zn	Mn	Fe	Al
7.38	0.26	0.05	0.013	0.007	0.19	0.25	Bal.

Figure 1 illustrates the overall fabrication process of the GNP/A356 Al composites. Based on the previous study [16], 0.3 wt.% GNPs amount is the optimum amount at the best performance for GNP/A356 aluminium composites. The GNP powder (0.3 wt. %) with purity of

>99% was purchased from Sigma-Aldrich, USA. 1 wt.% magnesium (Mg) powder was employed as a wetting agent. 400 g of A356 ingot was melted at 700 ℃ in a furnace with a holding time of 5 minutes before the temperature was reduced to 650 ℃. Then, GNP and Mg powder were injected into the molten metal and stirred at a speed of 500 rpm for 5 minutes. The mixture was subsequently poured into a preheated cylindrical steel mould.

The as-cast composite feedstock was reheated in an induction coil to a 50 % liquid fraction at 581 ℃ before being rammed into the mould with a 20 kN laboratory force with an 85 $mm.s^{-1}$ compression velocity. The temperature of the 50 % liquid fraction was obtained from the differential scanning calorimetry (DSC) graph, as shown in Figure 2. Subsequently, a T6 heat treatment was performed on the thixoformed composite. The T6 heat treatment process consisted of a solution treatment (540 °C for 8 hours), quenched in warm water (60 °C), and subsequent artificial ageing (160 °C for 4 hours). After being subjected to artificial ageing, the treated composite was cooled at room temperature.

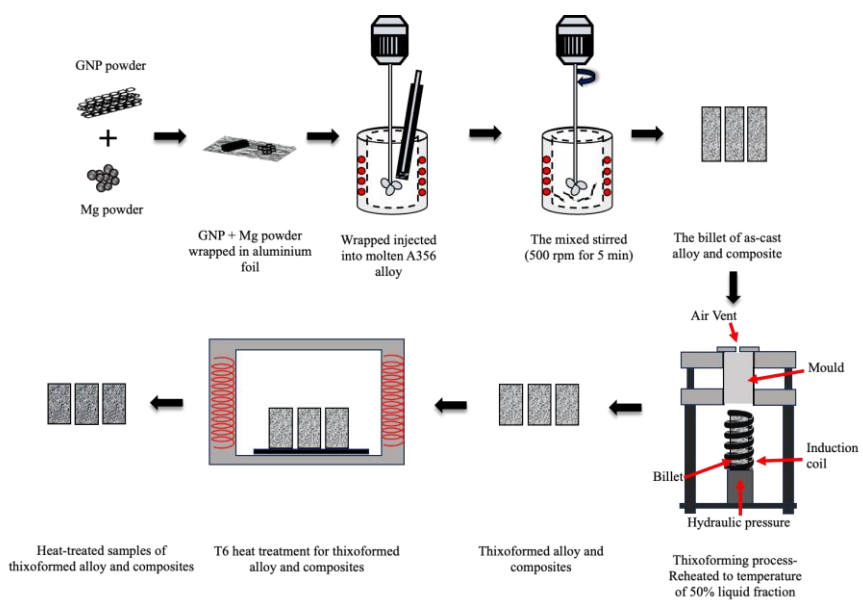

Figure 1: Diagram illustrating the GNP/A356 composites fabrication technique in this study. [is this proposed technique or referred from other?-This is the proposed technique to be used in this study]

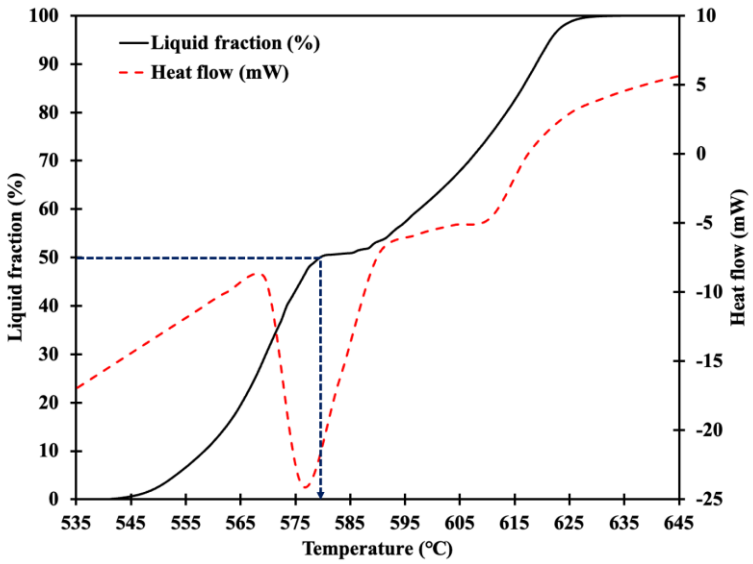

Figure 2: Profile of liquid fractions and DSC curve for A356 alloy.

2.2 Characterization

This study examined the microstructures of the as-cast, thixoformed, and heat-treated samples utilizing optical microscopy (OM) and field emission scanning electron microscopy (FESEM) with energy dispersive X-ray analysis (EDX). The samples underwent a grinding technique, polished with a diamond suspension, and etched with Keller's reagent for preparation standards. The identification of phases in the composite samples was carried out using X-ray diffraction (XRD). The experimental density of alloy and composites was obtained with five measurements and was identified using Archimedes' technique. A Vickers hardness instrument was used to investigate the hardness, with a 1 kgf load and 10 s dwell time.

2.3 Dry Sliding Wear Test

The wear rate was determined by employing the pin-on-disc method in dry sliding wear tests conducted following ASTM-G99 standards. The sliding distance of 3000 m, the sliding speed of 1 m/s, and a normal load of 50 N were the selected constant settings for the parameters in this study. The pin wear samples of alloy and composites were weighted before and after the wear test using a 0.0001g precise digital scale. The volume loss was calculated by mass loss (g) divided by experimental density (g/mm^3), while the specific wear rate was

measured using volume loss divided by the normal load (N) and sliding distance (m). Three-pin samples for each alloy and composite were tested for each parameter experiment to obtain reliable measurements. The friction force is continuously collected using cell load in the system of data acquisition during the wear test. FESEM was utilised to identify the wear mechanisms by evaluating the worn surface of the fabricated composite samples after the wear test.

3.0 RESULTS AND DISCUSSION

3.1 Microstructure of fabricated composites

Figure 3 depicts the optical micrographs of the A356 alloy and composite samples. The micrographs consist of two phases, which were the α-Al phase (bright areas) and the eutectic Si phase (dark areas). The application of stir-casting resulted in a non-dendritic structure, as shown in Figures 3 (a) and 3 (b). Figure 3(a) shows that the α-Al phase for as-cast A356 alloy was contained with a more rosette-like structure and coarser compared to the α-Al phase for as-cast GNP/A356 composites where the phase is more globular as shown in Figure 3(b).

Figure 3 (c) illustrates the transformation of the phase of α-Al in the GNP/A356 composite after the thixoforming process. The α-Al phase in the thixoformed composite becomes coarser with an irregular globular shape than the as-cast composite due to reheating process. The irregular globular structure was formed because of the presence of GNP in the composite. Furthermore, the eutectic Si in the thixoformed composite transforms into a fine fibrous structure instead of a coarse needle-like structure

Figure 3 (d) demonstrates the transformation of the Si eutectic phase after the T6 heat treatment process. The micrograph shows that heat treatment transformed the Si shape from fibrous eutectic Si to a spherical structure. A few researchers have reported a similar observation [17, 18], which indicates that the heat treatment process alters the needle-like microstructure of the Si eutectic into finely spheroid Si particles that are uniformly distributed throughout the alloy. The transformation to fine spheroid Si particles was one of the factors in the heat treatment process that strengthened the final product.

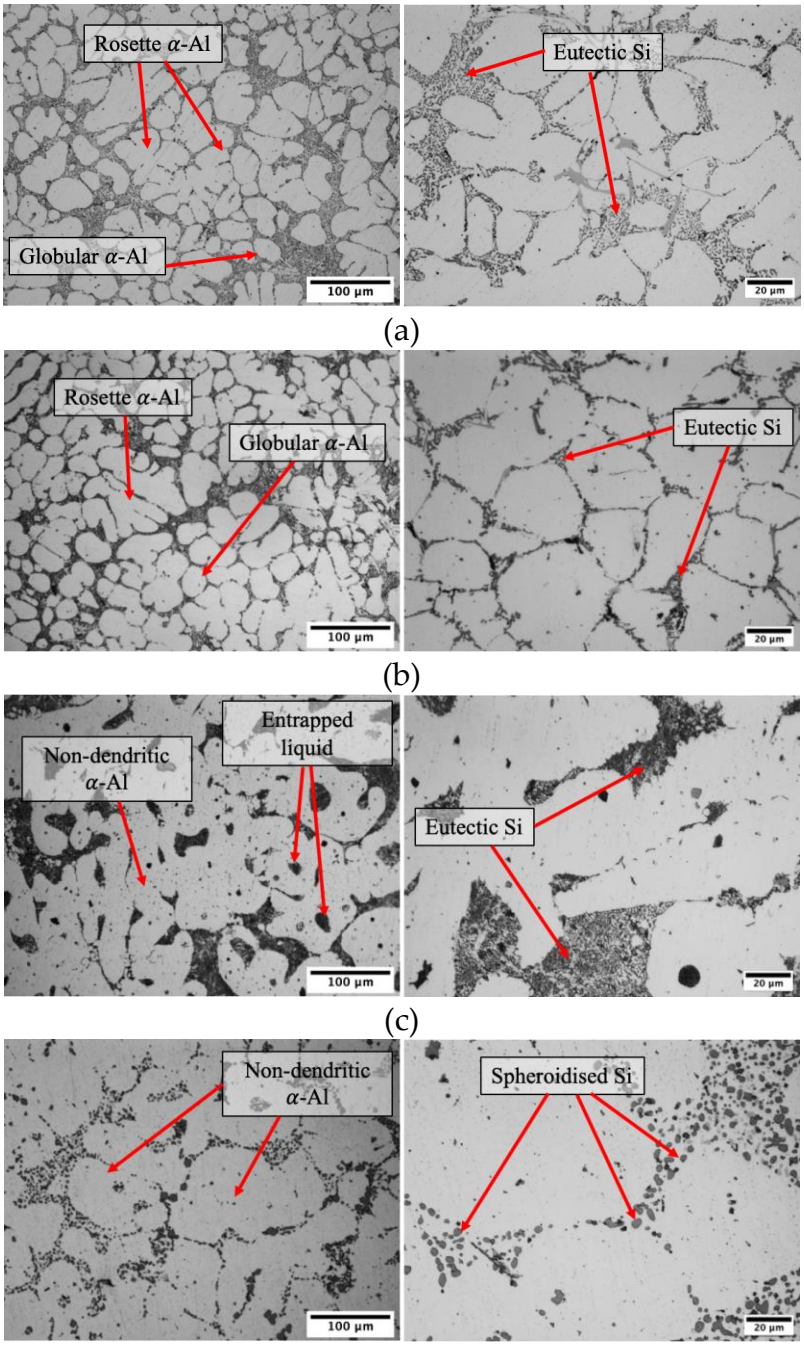

Caption for each image - center alignment

Figure 3: Optical microstructure of (a) as-cast A356 alloy, (b) as-cast GNP/A356 composite, (c) thixoformed GNP/A356 composite, and (d)

thixoformed-T6 GNP/A356 composite

Figure 4 presents the diffraction patterns of the composites obtained using different processes. The prominent diffraction peak in the XRD pattern was Al, followed by Si. However, the peak of GNP was not detected owing to its low content, and it was beyond the XRD equipment limitations [19].

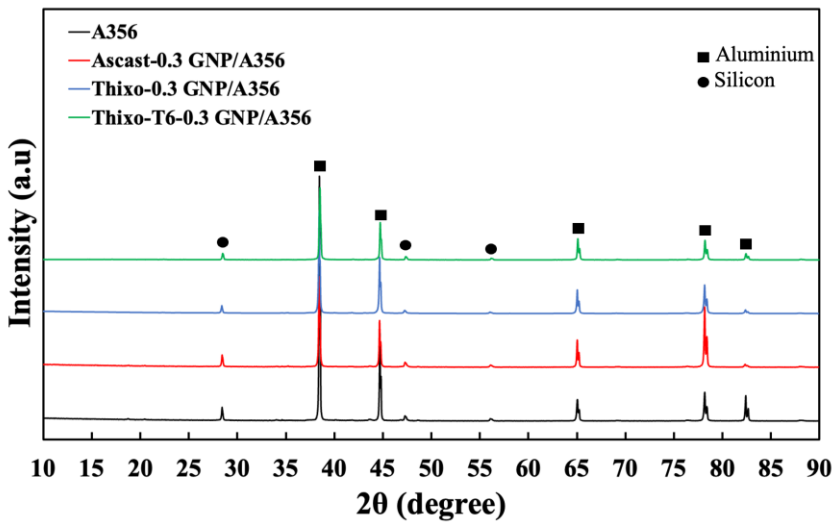

Figure 4: XRD patterns of A356 and the composite for different processes.

The FESEM and EDX analyses further explained the formation of compound intermetallic phases. Figures 5 (a) and (b) demonstrate the FESEM micrographs of the thixoformed and thixoformed-T6 composites, respectively. According to the EDX results, the scattering of C indicated the presence of reinforcement in the composite. Moreover, the EDX micrographs indicate that the peak for aluminium is the highest, along with several other notable peaks. This suggests that Al is the predominant component in the sample, with the other elements present at varying concentrations.

Furthermore, the EDX analysis identified the presence of β-Al5FeSi, as shown in Point A in Figure 5 (a) and Point C in Figure 5 (b). The amount of Fe was slightly higher in the thixoformed composites than in the thixoformed-T6 composites. On the other hand, the phase of π-Al8Si6Mg3Fe was detected as shown in Point B (Figure 5(a)) and Point D (Figure 5(b)) for the thixoformed 0.3 GNP/A356 composite and thixoformed-T6 0.3 GNP/A356 composite, respectively. Additionally,

the needle-like structure phase of π-Al8Si6Mg3Fe particles was fragmented into globular particles when subjected to the T6 heat treatment process, as shown in Point D.

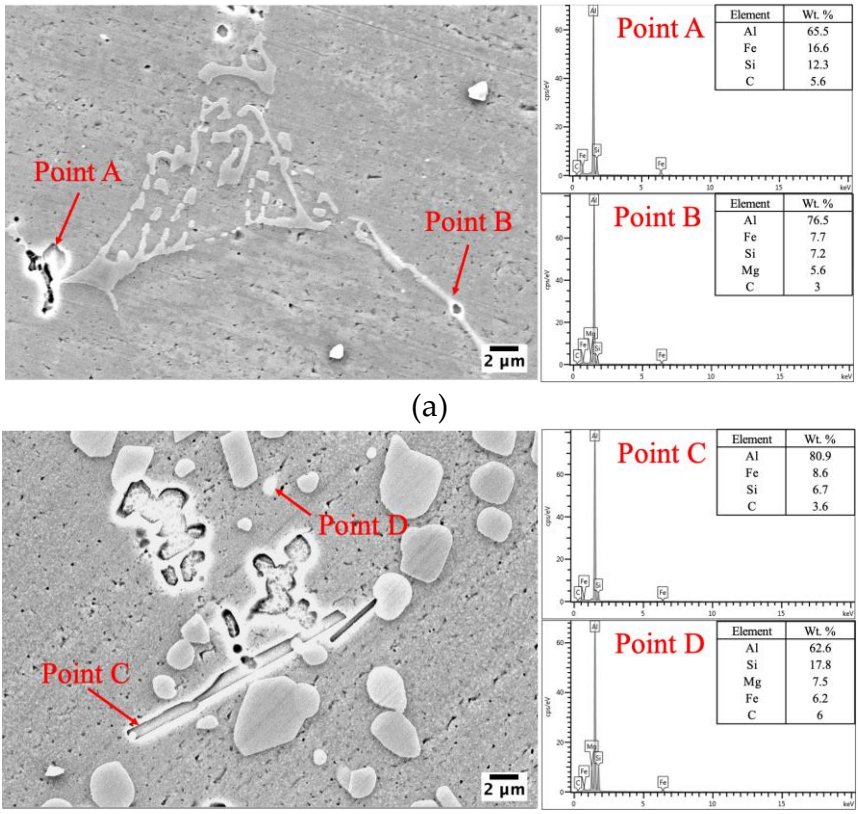

Caption for each image - center alignment

Figure 5: FESEM-EDX micrographs of (a) thixoformed 0.3 GNP/A356 composites and (b) thixoformed-T6 GNP/A356 composites. Point A and Point C: β-Al_5FeSi; Point B and Point D: π-$Al_8Si_6Mg_3Fe$.

3.2 Hardness properties of fabricated composite

The Vickers hardness and relative density of as-cast A356 and composites produced through subjected processes are illustrated in Figure 6. The thixo-T6 composite exhibited increased hardness and relative density hardness compared to the as-cast and thixoformed composites. The addition of GNPs in the composite materials can also be attributed to the observed improvement in hardness. Moreover, the increment in hardness of the composites can be ascribed to the development of an intermetallic phase

due to precipitation hardening and fine globular Si grains forming during the heat treatment process [20]. Accordingly, adding GNPs, applying thixoforming, and T6 heat treatment enhanced the hardness by approximately 70.5% compared to that of the A356 alloy. Furthermore, the notable enhancement in the hardness of the composite might be ascribed to the successful dispersion of GNPs in the composites during the production process.

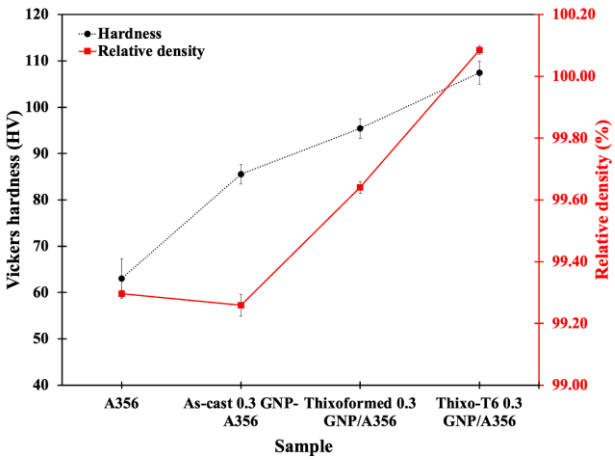

Figure 6: Hardness values of A356 and the composites.

3.3 Wear Behaviour

Fig. 7(a) illustrates the relationship between the volume wear loss and the samples at a normal load of 50 N. This shows that the volume wear loss decreased after the T6 heat treatment. Fig. 7(b) illustrates the plot of the specific wear rate for all samples. As shown in Fig. 7(b), the as-cast A356 alloy exhibits the highest specific wear rate. The formation of an adhesive between the surface contact and the inadequacy of load-bearing particles in the A356 alloy contributed to its high wear rate. In addition, the low hardness inhibits the ability of the alloy to resist deformation during sliding. Hence, the enhanced reduction in wear rate in the thixo-T6 composite sample can be ascribed to increased hardness, relative density, fine Si spheroidal particles, and GNPs as effective load-bearing particles [21].

Fig. 7(c) shows the average coefficient of friction (COF) results of

composites after thixoformed and heat-treated composites. The thixoformed composite sample showed the lowest COF compared with the thixo-T6 composite sample. However, the COF value of the thixo-T6 composite was still lower than those of the as-cast A356 alloy and composite.

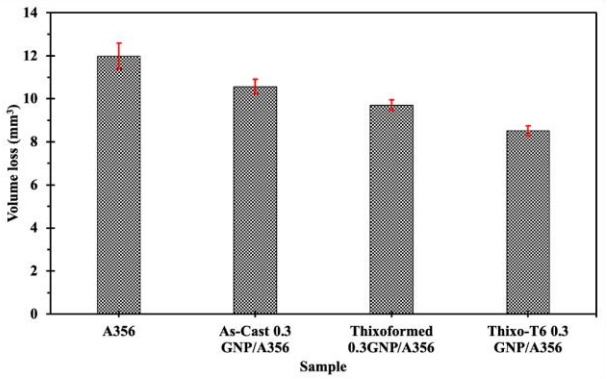

(a)

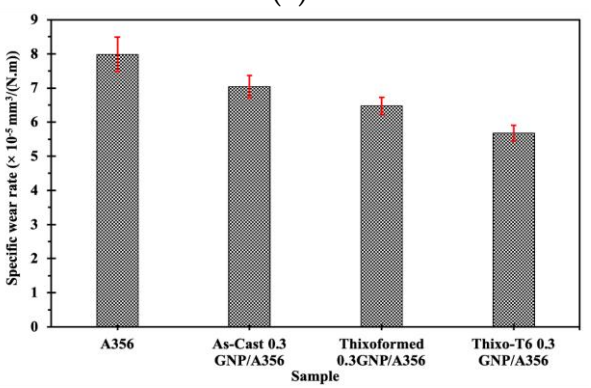

(b)

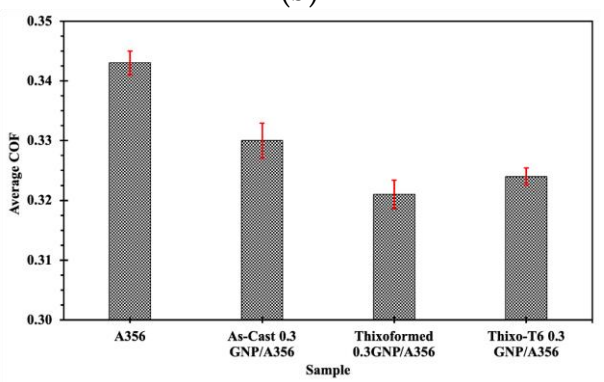

(c)

Caption for each image - center alignment

Figure 7: (a) Volume loss, (b) specific wear rate, and (c) average COF of the A356 alloy and composites.

Fig. 8 shows FESEM micrographs of the worn surface corresponding to the A356 alloy and composites after casting, thixoforming and T6 heat treatment process. Fig. 8(a) illustrates the worn surface of the A356 alloy, which was characterised by severe grooves on the worn surface. Craters and adhesive marks were also observed, which are typical of delamination wear. In contrast, fewer crates with grooves were detected on the worn surface of the as-cast composite, as shown in Fig. 8(b).

The application of the thixoforming process to the composite transformed its worn surface into an abrasive wear mechanism, as shown in Fig. 8(c). The presence of GNPs in sliding friction improves the self-lubricating properties, improving the worn surface [22] and subsequently reducing the wear rate of the fabricated composite. Meanwhile, Fig. 8(d) shows that the worn surface of the thixoformed-T6 composite exhibited grooves and adhesion, including material transfer. Therefore, abrasive and adhesive wear were dominant wear for the thixoformed-T6 composite.

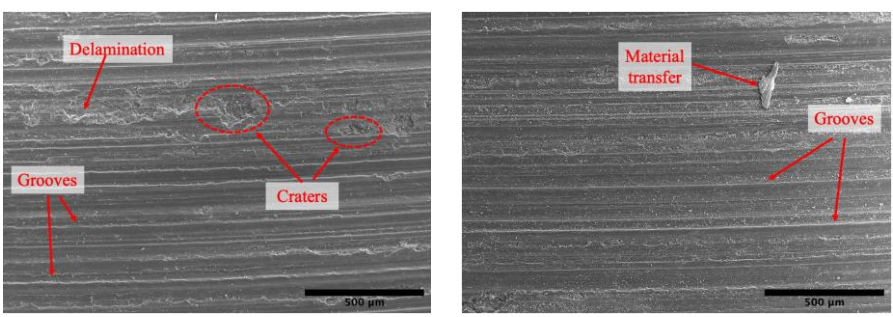

(a) (b)

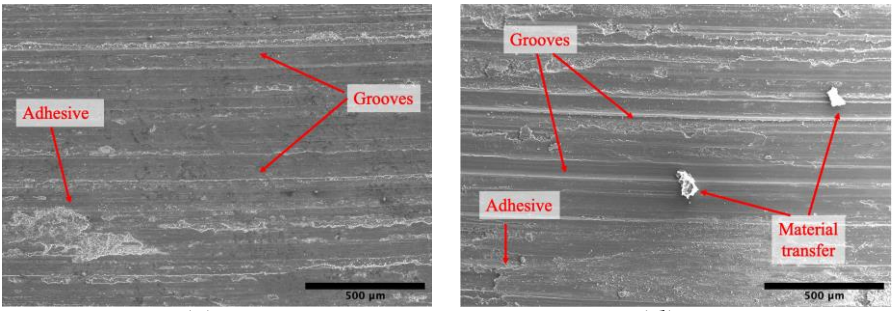

(c) (d)

Caption for each image - center alignment
Figure 8: FESEM images of the worn surface of (a) A356 alloy, (b) as-cast 0.3GNP/A356, (c) thixoformed 0.3GNP/A356 and (d) thixo-T6 0.3 GNP/A356.

4.0 CONCLUSION

The 0.3 % GNPs reinforced A356 matrix composites were developed by the semi-solid route and subsequent standard T6 heat treatment process. The impact of heat treatment process on the microstructure, hardness and dry sliding wear behaviour were examined. The standard process of T6 heat treatment significantly affected the transformation of eutectic Si from coarse needle-like to a spheroidal structure. The addition of GNPs, thixoforming, and heat treatment process offers an enhancement in the hardness, volume wear loss, specific wear rate, and COF of the thixoformed-T6 composite of the heat-treated composite by about 70.5 %, 28.9 %, 29 %, and 5.5 %, respectively, compared to the A356 alloy.

ACKNOWLEDGMENTS

The study is funded by the Ministry of Higher Education (MOHE) of Malaysia through the Fundamental Research Grant Scheme (FRGS), No. FRGS/1/2022/TK10/UTEM/02/18. The authors would also like to thank Universiti Teknikal Malaysia Melaka (UTeM) and Universiti Kebangsaan Malaysia (UKM) for supporting this study.

AUTHOR CONTRIBUTIONS

N.F.B.W. Anuar: Methodology, Investigations, Writing- Original Draft, Methodology, Conceptualization, Methodology; **M.Z. Omar**: Writing-

Review & Editing, Validation, Supervision; **M.S. Salleh**: Writing-Review & Editing, Validation, Supervision; **S.H Yahaya**: Writing-Review & Editing, Supervision; **S. Al-Zubaidi**: Writing-Reviewing and Editing.

CONFLICTS OF INTEREST

The manuscript has not been published elsewhere and has not been considered by the other journals. All authors have approved the review, and agreed with its submission, and we certify that there are no conflicts of interest in the manuscript.

REFERENCES

[1] S. Zhang, P. Wei, Z. Chen, B. Li, K. Huang, Y. Zou and B. Lu, "Graphene/ZrO_2/aluminum alloy composite with enhanced strength and ductility fabricated by laser powder bed fusion", *Journal of Alloys and Compounds*, vol. 910, p. 1-11, 2022.

[2] Z. Lin, Y. Su, C. Qiu, J. Yang, X. Chai, X. Liu, Q. Ouyang and D. Zhang, "Configuration effect and mechanical behavior of particle reinforced aluminum matrix composites", *Scripta Materialia*, vol. 224, p. 1-5, 2023.

[3] K.M. Mehta and V.J. Badheka, "Wear behavior of Al-6061-B4C surface composites fabricated by Friction stir processing using slot and hole method of reinforcement application", *Wear*, vol. 522, p. 1-9, 2023.

[4] S.K. Soni, Manimaran D, S.B. Thomas, and B. Thomas, "Microstructure and mechanical characterization of Al6061 based composite and nanocomposites prepared via conventional and ultrasonic-assisted melt-stirring techniques", *Materials Today Communications*, vol. 34, p. 1-15, 2023.

[5] V. Khalili, A. Heidarzadeh, S. Moslemi, and L. Fathyunes, "Production of Al6061 matrix composites with ZrO_2 ceramic reinforcement using a low-cost stir casting technique: Microstructure, mechanical properties, and electrochemical behavior", *Journal of Materials Research and Technology*, vol. 9, no. 6, pp. 15072–15086, 2020.

[6] A. Piasecki, P. Paczos, M. Tuliński, et al., "Microstructure, mechanical properties and tribological behavior of Cu-nano TiO_2-MWCNTs composite sintered materials", *Wear*, vol. 522, p. 1-16, 2023.

[7] H. Chang, J. Sun, G. Chen, B. Wang, L. Yang, J. Zhang and W. Tang, "Microstructure and properties of high-fraction graphite nanoflakes/6061Al matrix composites fabricated via spark plasma sintering", *Transactions of Nonferrous Metals Society of China*, vol. 31, no.

6, pp. 1550–1560, 2021.

[8] J. Yu, Q. Zhao, S. Huang, eY. Zhao, J. Lu, L. Dong and N. Tian, "Enhanced mechanical and tribological properties of graphene nanoplates reinforced TC21 composites using spark plasma sintering", *Journal of Alloys and Compounds*, vol. 873, p. 1-13, 2021.

[9] J. Leng, B. Ren, Y. Jin, Y. Zhu, and K. Wang, "Effects of graphene addition on the refinement of silicon phase in graphene/A356.2 composites", *Materials Letters*, vol. 292, p. 1-4, 2021.

[10] M.S. Hasan, A. Kordijazi, P.K. Rohatgi, and M. Nosonovsky, "Machine learning models of the transition from solid to liquid lubricated friction and wear in aluminum-graphite composites", *Tribology International*, vol. 165, p. 1-11, 2022.

[11] K. Shivalingaiah, V. Nagarajaiah, C.P. Selvan, S.T. Kariappa, N.G. Chandrashekarappa, A. Lakshmikanthan, M.P.G. Chandrashekarappa and E. Linul, "Stir casting process analysis and optimization for better properties in Al-MWCNT-GR-based hybrid composites", *Metals*, vol. 12, no. 8, p. 1-25, 2022.

[12] Z. Zheng, X. Zhang, M. Qian, J. Li, M. Imran, and L. Geng, "Ultra-high strength GNP/2024Al composite via thermomechanical treatment", *Journal of Materials Science & Technology*, vol. 108, pp. 164–172, 2022.

[13] Z. Jia, G. Zhou, H. Zhou, F. Liu, L. Ding, Y. Weng, K. Xiang and H. Zhao, "Effects of Cu content and heat treatment process on microstructures and mechanical properties of Al−Si−Mg−Mn−xCu cast aluminum alloys", *Transactions of Nonferrous Metals Society of China*, vol. 34, no. 3, pp. 737–754, 2024.

[14] Y. Wang and T. Monetta, "Systematic study of preparation technology, microstructure characteristics and mechanical behaviors for SiC particle-reinforced metal matrix composites", *Journal of Materials Research and Technology*, vol. 25, pp. 7470–7497, 2023.

[15] K. Nithesh, M.C. Gowrishankar, R. Nayak, and S. Sharma, "Effect of light weight reinforcement and heat treatment process parameters on morphological and wear aspects of hypoeutectic Al-Si based composites - a critical review", *Journal of Materials Research and Technology*, vol. 15, pp. 4272–4292, 2021.

[16] A. Md Ali, M.Z. Omar, M.S. Salleh, H. Hashim, I.F. Mohamed, and N.F.B. Wakhi Anuar, "Mechanical behaviour and morphology of thixoformed aluminium alloy reinforced by graphene", *Materials*, vol. 15, no. 19, p. 1-15, 2022.

[17] M.A. Abdelgnei, M.Z. Omar, M.J. Ghazali, and M.N. Mohammed, "Microstructure evaluation and mechanical properties of thixoformed Ai–5.7Si–2Cu–0.3Mg aluminum alloys", *International Journal of Metalcasting*. vol. 16, no. 1, pp. 370–384, 2022.

[18] I. V. Gomes, J. Grilo, V.H. Carneiro, and H. Puga, "Impact of the ultrasonic-assisted casting of an AlSi7Mg alloy on T6 heat treatment", *Metals*. vol. 13, no. 2, p. 1-13, 2023.

[19] R. Roy and S. Mondal, "Microstructure and properties of nanocomposites with graphene-reinforced aluminum matrix", *Metal Science and Heat Treatment*, vol. 65, no. 1–2, pp. 42–46, 2023.

[20] M.E. Turan, F. Aydin, Y. Sun, H. Zengin, and Y. Akinay, "Wear resistance and tribological properties of GNPs and MWCNT reinforced AlSi18CuNiMg alloys produced by stir casting", *Tribology International*, vol. 164, p. 1-15, 2021.

[21] A. Lakshmikanthan, T.R. Prabhu, U.S. Babu, P.G. Koppad, M. Gupta, M. Krishna and S. Bontha, "The effect of heat treatment on the mechanical and tribological properties of dual size SiC reinforced A357 matrix composites", *Journal of Materials Research and Technology*, vol. 9, no. 3, pp. 6434–6452, 2020.

[22] J. Bao, Z. Liu, Y. Yang, and H. Yan, "Influence of T6 heat treatment on the microstructure and tribological properties of ADC12-GNPs composites", *Diamond and Related Materials*, vol. 140, p. 1-11, 2023.